Supporting Information

Influence of Solvent in Solvothermal Syntheses: Change of Nuclearity in Mixed Valence $Co^{II/III}$ Complexes of a O-Donor-rich Schiff Base Ligand

Suman Kr Dey,[†] Partha Mitra,[‡] and Arindam Mukherjee*[,†]

[†]Department of Chemical Sciences, and [‡]Department of Physical Sciences, Indian Institute of Science Education and Research Kolkata, Mohanpur-741246, India

Table of Contents

Table S1 Selected bond distances (Å) and angles (deg) for **2**-**4**.

2		**3**		**4**	
Co(1)…Co(3)	2.9426(10)	Co(1)…Co(3)	3.051(1)	Co(1)…Co(2)	2.9992(6)
Co(2)…Co(3)	2.9843(11)	Co(2)…Co(4)	3.056(1)	Co(2)…Co(2A)	3.4621(6)
Co(3)…Co(4)	2.9906(11)	Co(3)…Co(4)	3.126(1)	Co(2)…Co(2B)	4.8962(6)
		Co(3)…Co(5)	2.832(1)	Co(2)…Co(3)	2.9577(6)
Co(1)-O(1)	1.881(3)	Co(4)…Co(5)	2.815(1)		
Co(1)-O(2)	1.967(3)			Co(1)-O(5)	1.872(2)
Co(1)-O(5)	1.885(3)	Co(1)-O(1)	1.884(4)	Co(1)-O(1)	1.874(2)
Co(1)-O(6)	1.964(3)	Co(1)-O(2)	1.921(4)	Co(1)-N(2)	1.899(3)
Co(1)-N(1)	1.904(4)	Co(1)-O(5)	1.879(4)	Co(1)-N(1)	1.903(3)
Co(1)-N(2)	1.913(4)	Co(1)-O(6)	1.952(4)	Co(1)-O(2)	1.929(2)
Co(2)-O(9)	2.116(4)	Co(1)-N(1)	1.907(4)	Co(1)-O(6)	1.940(2)
Co(2)-O(3)	2.006(3)	Co(1)-N(2)	1.914(4)	Co(2)-O(6)	2.031(2)
Co(2)-O(6)	2.243(3)	Co(2)-O(9)	1.895(4)	Co(2)-O(3)	2.033(2)
Co(2)-O(10)	2.190(4)	Co(2)-O(10)	1.956(4)	Co(2)-O(2)	2.055(2)
Co(2)-O(11)	2.089(4)	Co(2)-O(13)	1.881(4)	Co(2)-O(7)	2.088(2)
Co(2)-N(6)	2.026(4)	Co(2)-O(14)	1.935(4)	Co(2)-O(7A)	2.105(2)
Co(3)-O(2)	1.948(3)	Co(2)-N(3)	1.902(4)	Co(2)-Cl(1)	2.7032(7)
Co(3)-O(3)	1.898(3)	Co(2)-N(4)	1.914(5)	Co(3)-O(7B)	2.085(2)
Co(3)-O(6)	1.942(3)	Co(3)-O(2)	2.014(4)	Co(3)-O(7C)	2.085(2)
Co(3)-O(7)	1.903(4)	Co(3)-O(3)	2.146(4)	Co(3)-O(7)	2.085(2)
Co(3)-N(4)	1.904(4)	Co(3)-O(6)	2.145(4)	Co(3)-O(7A)	2.085(2)
Co(3)-N(5)	1.908(4)	Co(3)-O(7)	2.102(4)	Co(3)-Cl(2)	2.3268(17)
Co(4)-O(2)	2.251(4)	Co(3)-O(15)	2.056(4)	Cl(1)-Co(2B)	2.7032(7)
Co(4)-O(13)	2.163(4)	Co(3)-O(18)	2.027(4)	Cl(1)-Co(2C)	2.7032(7)
Co(4)-O(7)	2.004(3)	Co(4)-O(3)	2.055(4)	Cl(1)-Co(2A)	2.7032(7)
Co(4)-O(12)	2.127(4)	Co(4)-O(10)	2.131(4)		
Co(4)-O(14)	2.074(4)	Co(4)-O(11)	2.067(4)	O(6)-Co(2)-O(3)	91.71(9)
Co(4)-N(3)	2.036(4)	Co(4)-O(14)	2.039(4)	O(6)-Co(2)-O(2)	79.40(8)
		Co(4)-O(15)	2.129(4)	O(3)-Co(2)-O(2)	89.53(9)
O(6)-Co(1)-O(2)	81.86(13)	Co(4)-O(17)	2.020(4)	O(6)-Co(2)-O(7)	95.55(8)
O(5)-Co(1)-O(2)	93.45(14)	Co(5)-O(3)	2.103(4)	O(3)-Co(2)-O(7)	172.39(9)
O(5)-Co(1)-O(6)	174.70(15)	Co(5)-O(6)	2.086(4)	O(2)-Co(2)-O(7)	94.05(8)
O(5)-Co(1)-N(1)	87.12(15)	Co(5)-O(10)	2.076(4)	O(6)-Co(2)-O(7A)	107.74(8)
O(5)-Co(1)-N(2)	94.64(15)	Co(5)-O(15)	2.120(4)	O(3)-Co(2)-O(7A)	89.66(8)
O(1)-Co(1)-O(2)	174.46(14)	Co(5)-O(19)	2.132(4)	O(2)-Co(2)-O(7A)	172.83(8)
O(1)-Co(1)-O(6)	93.29(14)	Co(5)-O(20)	2.127(4)	O(7)-Co(2)-O(7A)	85.95(11)
O(1)-Co(1)-O(5)	91.51(15)			O(5)-Co(1)-O(1)	90.59(10)
O(1)-Co(1)-N(1)	94.48(16)	O(5)-Co(1)-O(6)	176.36(18)	O(5)-Co(1)-N(2)	95.50(10)
O(1)-Co(1)-N(2)	87.13(16)	O(5)-Co(1)-O(2)	91.96(17)	O(1)-Co(1)-N(2)	88.86(10)
N(1)-Co(1)-O(2)	83.32(15)	O(5)-Co(1)-O(1)	91.79(18)	O(5)-Co(1)-N(1)	86.36(11)
N(1)-Co(1)-O(6)	94.74(15)	O(5)-Co(1)-N(2)	94.72(17)	O(1)-Co(1)-N(1)	95.40(10)
N(1)-Co(1)-N(2)	177.59(17)	O(5)-Co(1)-N(1)	86.24(17)	N(2)-Co(1)-N(1)	175.34(11)
N(2)-Co(1)-O(2)	94.92(16)	O(2)-Co(1)-O(6)	84.64(16)	O(5)-Co(1)-O(2)	92.45(9)
N(2)-Co(1)-O(6)	83.37(15)	O(1)-Co(1)-O(6)	91.61(17)	O(1)-Co(1)-O(2)	176.86(10)
O(9)-Co(2)-O(6)	90.83(12)	O(1)-Co(1)-O(2)	176.24(17)	N(2)-Co(1)-O(2)	91.64(10)
O(9)-Co(2)-O(10)	60.62(13)	O(1)-Co(1)-N(2)	86.20(18)	N(1)-Co(1)-O(2)	84.00(10)
O(3)-Co(2)-O(9)	156.46(14)	O(1)-Co(1)-N(1)	95.46(18)	O(5)-Co(1)-O(6)	177.24(10)
O(3)-Co(2)-O(6)	71.14(12)	N(2)-Co(1)-O(6)	84.21(17)	O(1)-Co(1)-O(6)	92.12(10)
O(3)-Co(2)-O(10)	107.46(13)	N(2)-Co(1)-O(2)	93.19(17)	N(2)-Co(1)-O(6)	84.06(10)
O(3)-Co(2)-O(11)	97.76(14)	N(1)-Co(1)-O6	94.73(17)	N(1)-Co(1)-O(6)	93.87(10)
O(3)-Co(2)-N(6)	86.53(15)	N(1)-Co(1)-O(2)	85.09(17)	O(2)-Co(1)-O(6)	84.85(9)
O(10)-Co(2)-O(6)	102.21(12)	N(1)-Co(1)-N(2)	178.06(19)	O(7B)-Co(3)-O(7C)	86.53(3)
O(11)-Co(2)-O(9)	99.91(14)	N(3)-Co(2)-O(14)	92.89(17)	O(7B)-Co(3)-O(7)	86.53(3)
O(11)-Co(2)-O(6)	168.90(13)	N(3)-Co(2)-O(10)	83.91(17)	O(7C)-Co(3)-O(7)	151.50(12)
O(11)-Co(2)-O(10)	80.93(14)	N(3)-Co(2)-N(4)	177.97(19)	O(7B)-Co(3)-O(7A)	151.50(12)
N(6)-Co(2)-O(9)	106.27(15)	O(14)-Co(2)-O(10)	84.79(16)	O(7C)-Co(3)-O(7A)	86.53(3)
N(6)-Co(2)-O(6)	81.82(14)	O(9)-Co(2)-N(3)	94.51(17)	O(7)-Co(3)-O(7A)	86.53(3)

N(6)-Co(2)-O(10)	166.01(15)	O(9)-Co(2)-O(14)	91.07(17)	O(7B)-Co(3)-Cl(2)	104.25(6)
N(6)-Co(2)-O(11)	97.68(15)	O(9)-Co(2)-O(10)	175.48(17)	O(7C)-Co(3)-Cl(2)	104.25(6)
O(3)-Co(3)-O(2)	96.42(14)	O(9)-Co(2)-N(4)	86.51(17)	O(7)-Co(3)-Cl(2)	104.25(6)
O(3)-Co(3)-O(6)	80.40(14)	O(13)-Co(2)-N(3)	86.72(18)	O(7A)-Co(3)-Cl(2)	104.25(6)
O(3)-Co(3)-O(7)	175.80(15)	O(13)-Co(2)-O(14)	176.70(17)	Co(2A)-Cl(1)-Co(2)	79.64(2)
O(3)-Co(3)-N(4)	94.21(16)	O(13)-Co(2)-O(10)	91.91(17)	Co(2B)-Cl(1)-Co(2C)	79.64(2)
O(3)-Co(3)-N(5)	88.58(16)	O(13)-Co(2)-O(9)	92.23(17)	Co(2)-Cl(1)-Co(2B)	129.82(5)
O(6)-Co(3)-O(2)	82.90(13)	O(13)-Co(2)-N(4)	95.00(18)	Co(2A)-Cl(1)-Co(2C)	129.82(5)
O(7)-Co(3)-O(2)	80.34(14)	N(4)-Co(2)-O(14)	85.33(17)	Co(2)-Cl(1)-Co(2A)	79.64(2)
O(7)-Co(3)-O(6)	96.48(14)	N(4)-Co(2)-O(10)	94.94(17)	Co(2C)-Cl(1)-Co(2A)	79.64(2)
O(7)-Co(3)-N(4)	88.56(16)	O(7)-Co(3)-O(3)	166.11(16)	Co(1)-O(2)-Co(2)	97.62(9)
O(7)-Co(3)-N(5)	94.32(16)	O(7)-Co(3)-O(6)	87.76(15)	Co(1)-O(6)-Co(2)	98.07(9)
N(4)-Co(3)-O(2)	91.23(15)	O(6)-Co(3)-O(3)	80.41(15)	Co(3)-O(7)-Co(2)	90.26(8)
N(4)-Co(3)-O(6)	171.49(16)	O(15)-Co(3)-O(7)	99.49(16)	Co(3)-O(7)-Co(2A)	89.80(8)
N(4)-Co(3)-N(5)	95.18(17)	O(15)-Co(3)-O(3)	72.36(15)	Co(2)-O(7)-Co(2A)	111.32(9)
N(5)-Co(3)-O(2)	171.57(15)	O(15)-Co(3)-O(6)	84.89(15)		
N(5)-Co(3)-O(6)	91.28(15)	O(2)-Co(3)-O(7)	92.43(16)		
O(13)-Co(4)-O(2)	99.27(13)	O(2)-Co(3)-O(3)	92.12(15)		
O(7)-Co(4)-O(2)	71.18(13)	O(2)-Co(3)-O(6)	77.59(15)		
O(7)-Co(4)-O(13)	106.80(14)	O(2)-Co(3)-O(15)	158.39(16)		
O(7)-Co(4)-O(12)	159.46(16)	O(2)-Co(3)-O(18)	100.74(17)		
O(7)-Co(4)-O(14)	99.91(16)	O(18)-Co(3)-O(7)	92.02(16)		
O(7)-Co(4)-N(3)	86.00(15)	O(18)-Co(3)-O(3)	100.01(16)		
O(12)-Co(4)-O(2)	93.95(14)	O(18)-Co(3)-O(6)	178.31(16)		
O(12)-Co(4)-O(13)	60.57(14)	O(18)-Co(3)-O(15)	96.80(17)		
O(14)-Co(4)-O(2)	170.75(15)	Co(5)-O(3)-Co(3)	83.59(13)		
O(14)-Co(4)-O(13)	85.51(16)	Co(4)-O(3)-Co(5)	85.22(14)		
O(14)-Co(4)-O(12)	95.29(17)	Co(4)-O(3)-Co(3)	96.17(15)		
N(3)-Co(4)-O(2)	81.74(15)	O(3)-Co(4)-O(11)	101.46(16)		
N(3)-Co(4)-O(13)	166.85(16)	O(3)-Co(4)-O(15)	72.73(15)		
N(3)-Co(4)-O(12)	106.32(16)	O(3)-Co(4)-O(10)	84.25(15)		
N(3)-Co(4)-O(14)	95.42(17)	O(11)-Co(4)-O(15)	168.96(16)		
Co(1)-O(2)-Co(4)	128.09(15)	O(11)-Co(4)-O(10)	88.34(15)		
Co(3)-O(2)-Co(1)	97.47(14)	O(15)-Co(4)-O(10)	81.79(15)		
Co(3)-O(2)-Co(4)	90.54(13)	O(14)-Co(4)-O(3)	158.87(16)		
Co(3)-O(3)-Co(2)	99.69(14)	O(14)-Co(4)-O(11)	89.39(16)		
Co(1)-O(6)-Co(2)	127.23(16)	O(14)-Co(4)-O(15)	93.37(15)		
Co(3)-O(6)-Co(1)	97.77(13)	O(14)-Co(4)-O(10)	77.94(15)		
Co(3)-O(6)-Co(2)	90.69(12)	O(17)-Co(4)-O(3)	98.69(17)		
Co(3)-O(7)-Co(4)	99.86(15)	O(17)-Co(4)-O(11)	93.52(17)		
		O(17)-Co(4)-O(15)	96.62(17)		
		O(17)-Co(4)-O(14)	98.68(17)		
		O(17)-Co(4)-O(10)	176.13(17)		
		O(3)-Co(5)-O(15)	71.98(15)		
		O(3)-Co(5)-O(20)	112.19(16)		
		O(3)-Co(5)-O(19)	72.23(16)		
		O(6)-Co(5)-O(3)	82.79(14)		
		O(6)-Co(5)-O(15)	84.81(15)		
		O(6)-Co(5)-O(20)	99.19(16)		
		O(6)-Co(5)-O(19)	93.25(15)		
		O(15)-Co(5)-O(20)	174.46(16)		
		O(15)-Co(5)-O(19)	114.45(16)		
		O(10)-Co(5)-O(3)	84.44(15)		
		O(10)-Co(5)-O(6)	164.74(15)		
		O(10)-Co(5)-O(15)	83.31(15)		
		O(10)-Co(5)-O(20)	93.36(16)		
		O(10)-Co(5)-O(19)	100.37(16)		
		O(20)-Co(5)-O(19)	61.71(16)		
		Co(1)-O(6)-Co(5)	134.04(19)		
		Co(1)-O(6)-Co(3)	96.13(15)		
		Co(5)-O(6)-Co(3)	84.01(14)		

	Co(5)-O(15)-Co(4) 83.00(14) Co(3)-O(15)-Co(5) 85.39(15) Co(3)-O(15)-Co(4) 96.66(15) Co(2)-O(14)-Co(4) 100.46(17) Co(2)-O(10)-Co(5) 131.55(19) Co(2)-O(10)-Co(4) 96.69(16) Co(5)-O(10)-Co(4) 84.00(14) Co(1)-O(2)-Co(3) 101.63(17)	

Symmetry transformations used to generate equivalent atoms: A -y+1/2, x, z ; B y, -x+1/2, z; C -x+1/2, -y+1/2, z.

Table S2 The bond valence sum calculation for **2-4**

	2		**3**		**4**	
Co-site	Co(II)	Co(III)	Co(II)	Co(III)	Co(II)	Co(III)
Co(1)	3.61	3.34	3.65	3.39	3.77	3.43
Co(2)	2.06	1.87	3.59	3.27	1.9	1.68
Co(3)	3.62	3.30	1.87	1.64	--	--
Co(4)	2.07	1.88	2.03	1.78	--	--
Co(5)	--	--	2.03	1.79	--	--

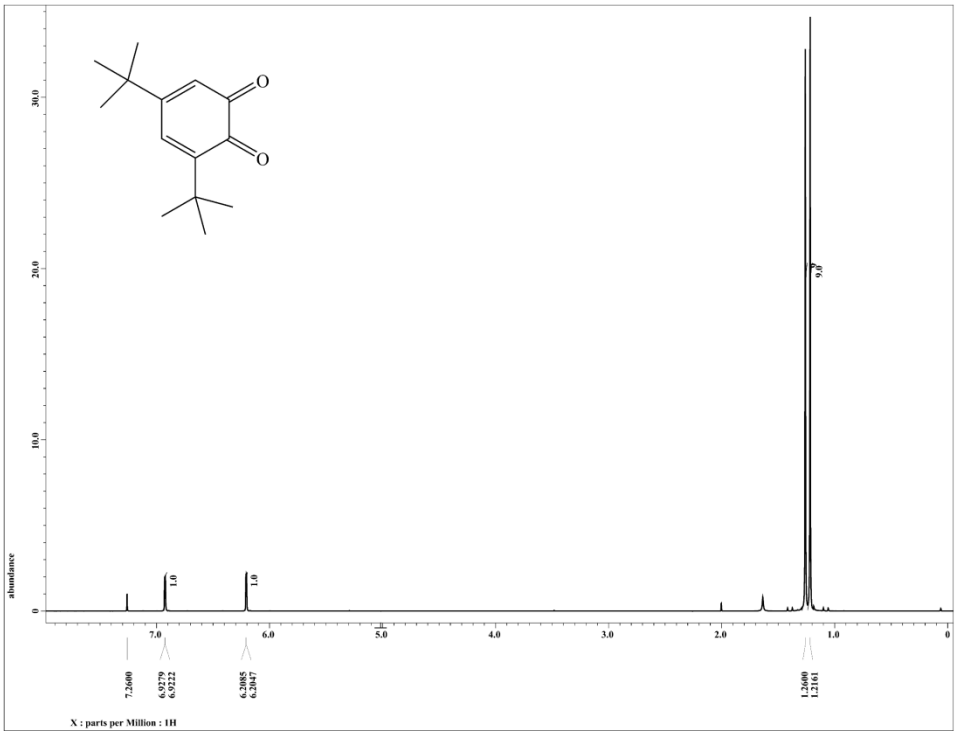

Figure S1. ^{1}H NMR of DTBQ in $CDCl_3$ obtained after catalytic study using complex **3**.

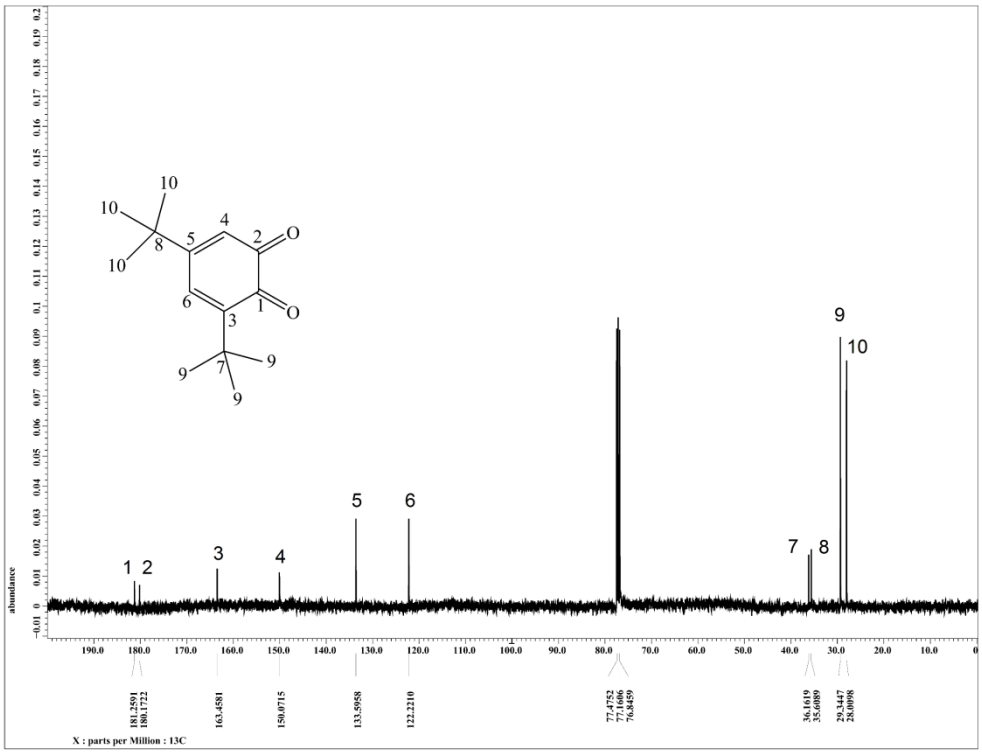

Figure S2. ^{13}C NMR of DTBQ in $CDCl_3$ obtained after catalytic study using complex **3**.

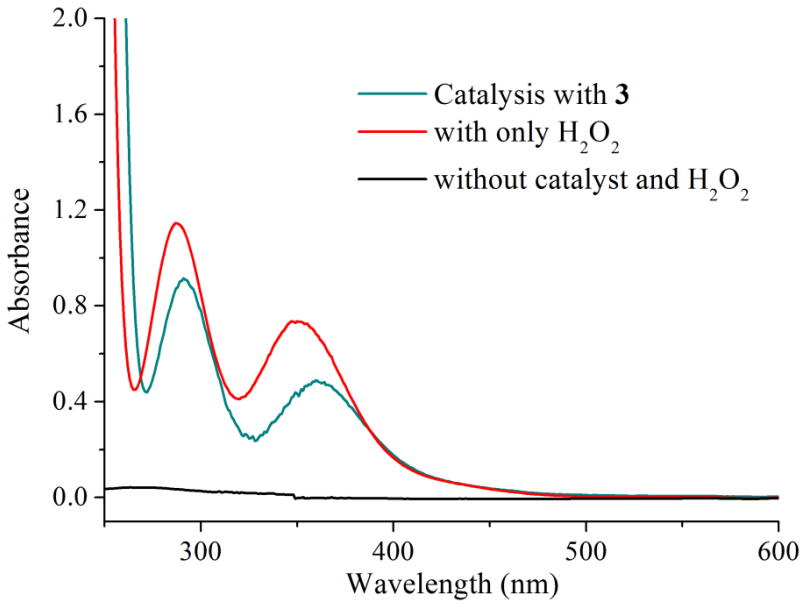

Figure S3. UV-Vis spectra of hydrogen peroxide detection test showing characteristic peak of I_3^- after DTBC oxidation with catalyst **3**. The spectrum for control and using H_2O_2 as standard is also shown.

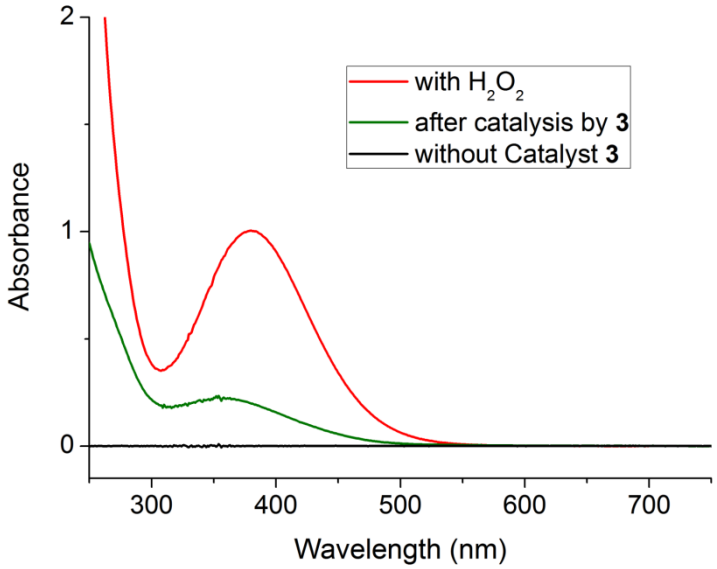

Figure S4. UV-Vis spectra of hydrogen peroxide detection test showing characteristic peak at 370 nm for the generation of Ti(IV)-peroxo complex by H_2O_2 in presence of potassium titanium(IV) oxalate. Similar characteristic peak was observed for DTBC oxidation by complex **3** demonstrating production of hydrogen peroxide during DTBC oxidation.

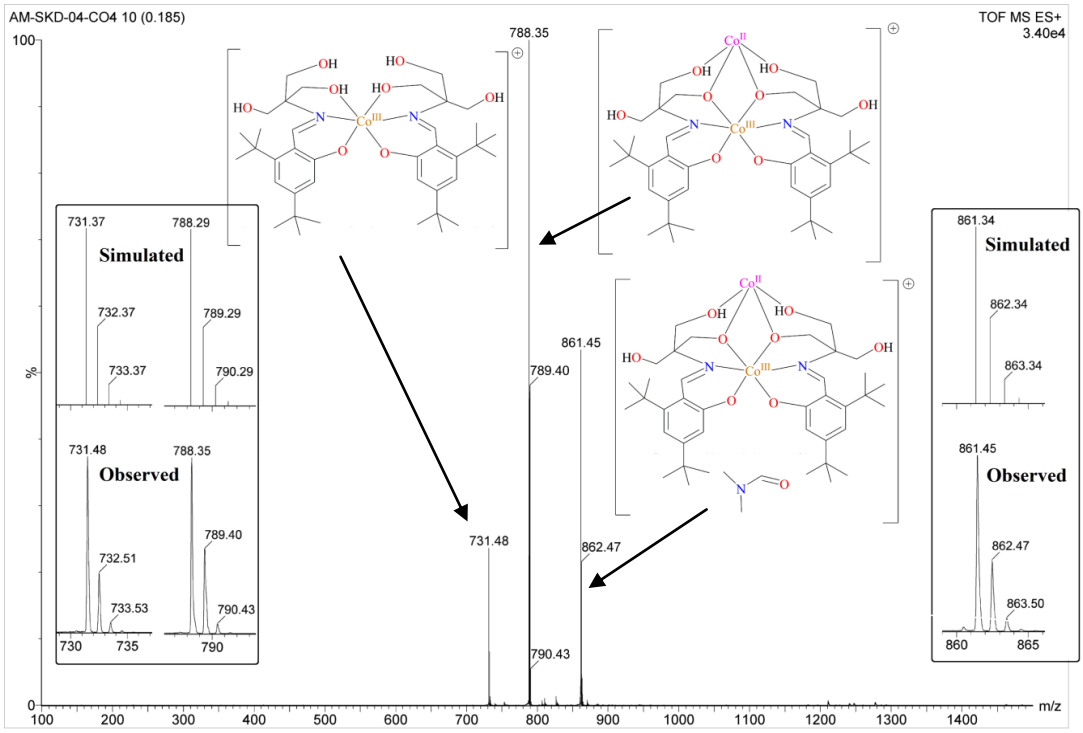

Figure S5. ESI-MS (+ve ion mode) of Complex **2** in methanol with 1% DMF. Inset showing isotopic distribution of the assign peaks.

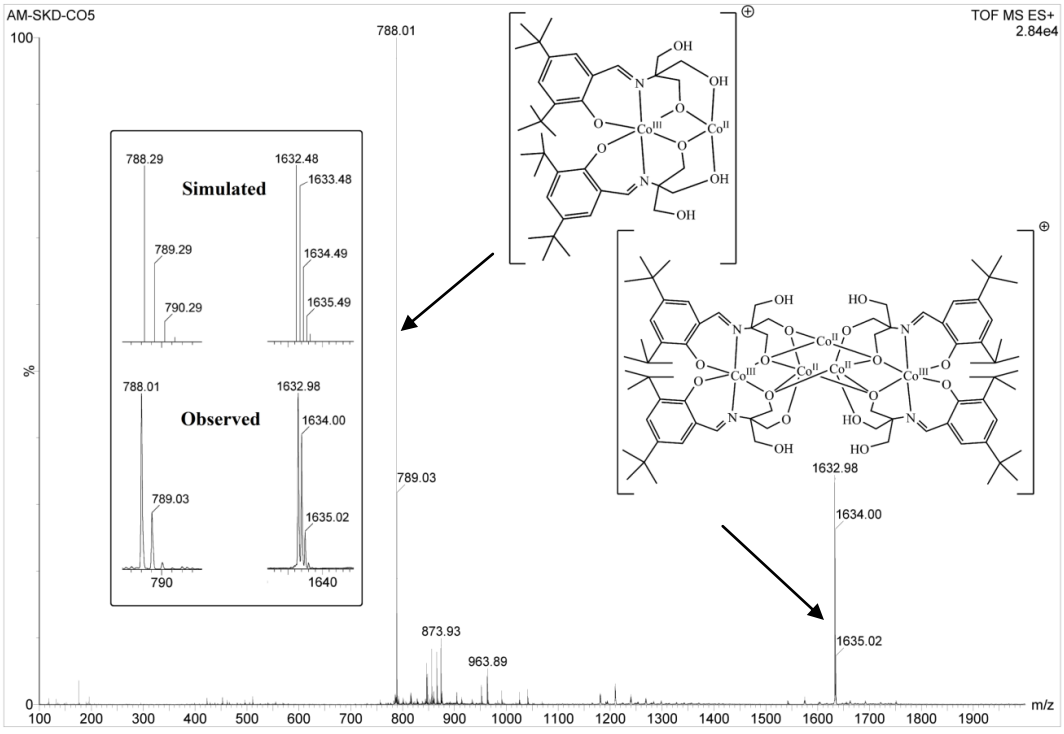

Figure S6. ESI-MS (+ve ion mode) of Complex **3** in methanol. Inset showing isotopic distribution of the assign peaks.

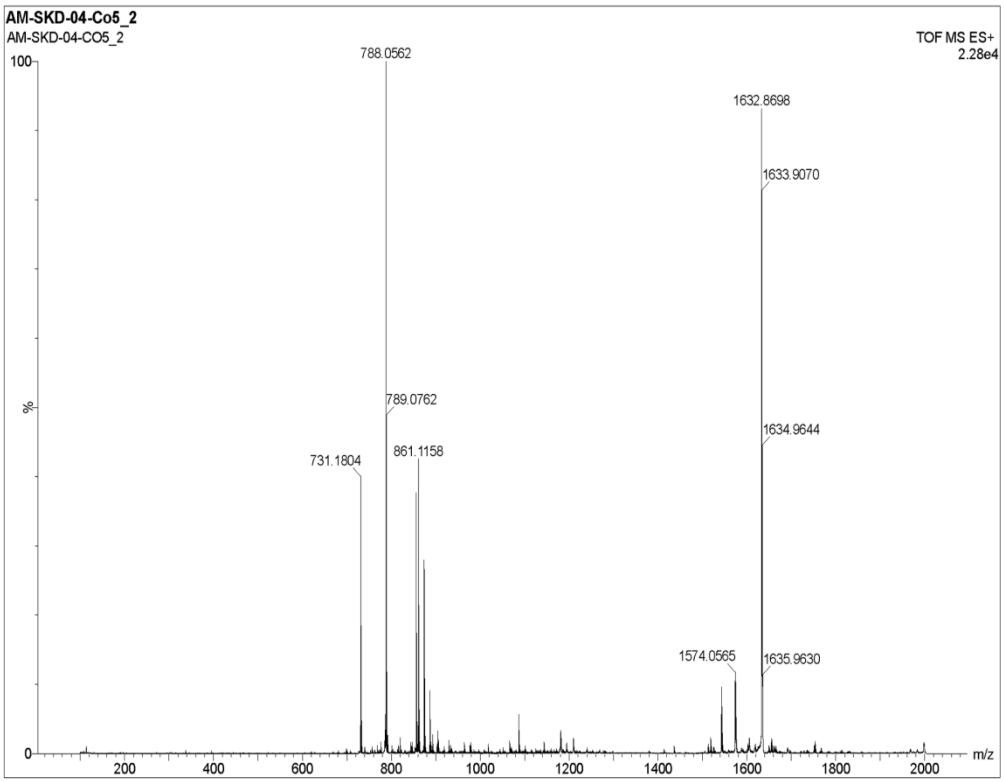

Figure S7. ESI-MS (+ve ion mode) of complex **3** in methanol after 12 h of solution preparation.

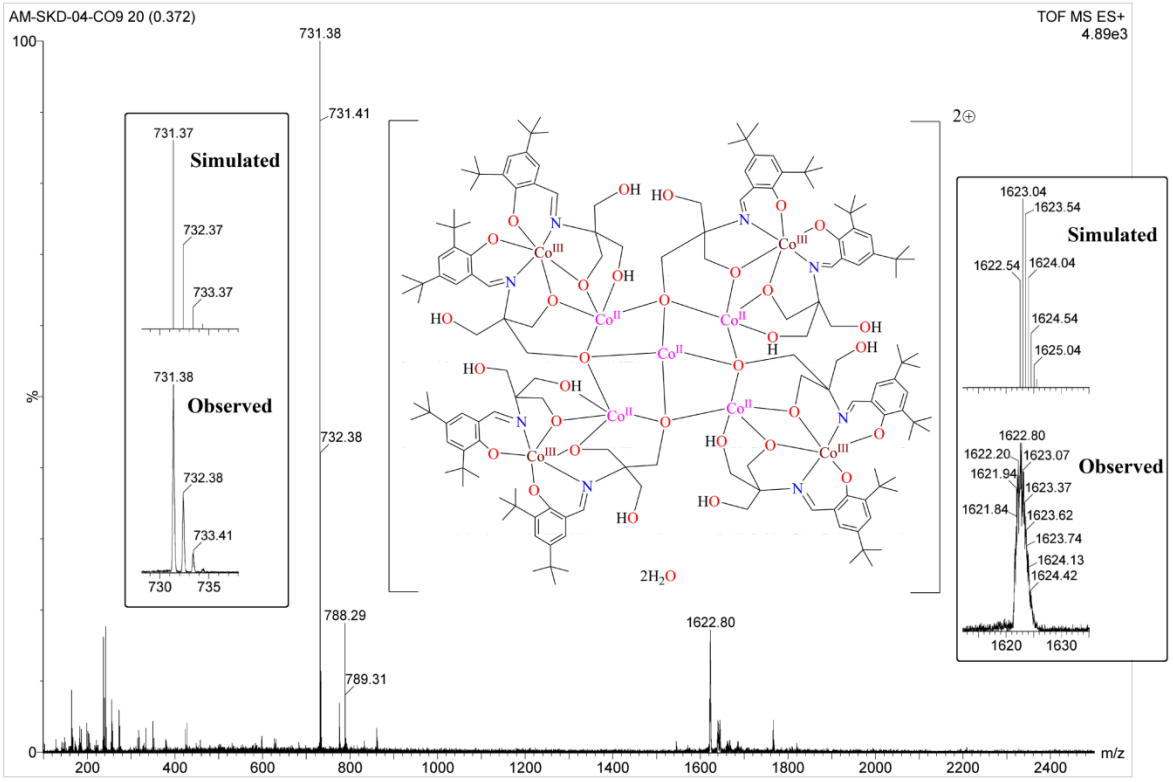

Figure S8. ESI-MS (+ve ion mode) of Complex **4** in acetonitrile with 1% DMF. Inset showing isotopic distribution of the assign peaks.

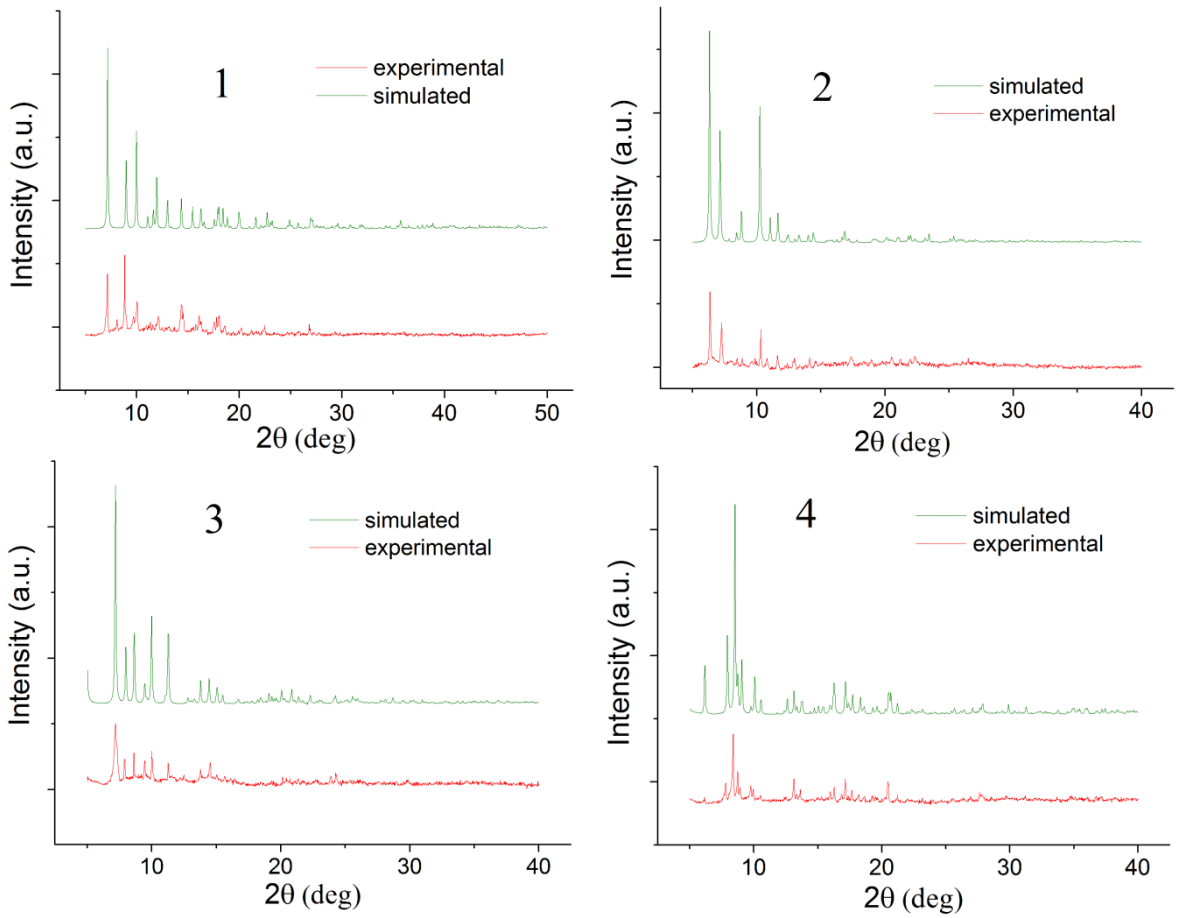

Figure S9. Simulated and experimental PXRD patterns of **1-4.**

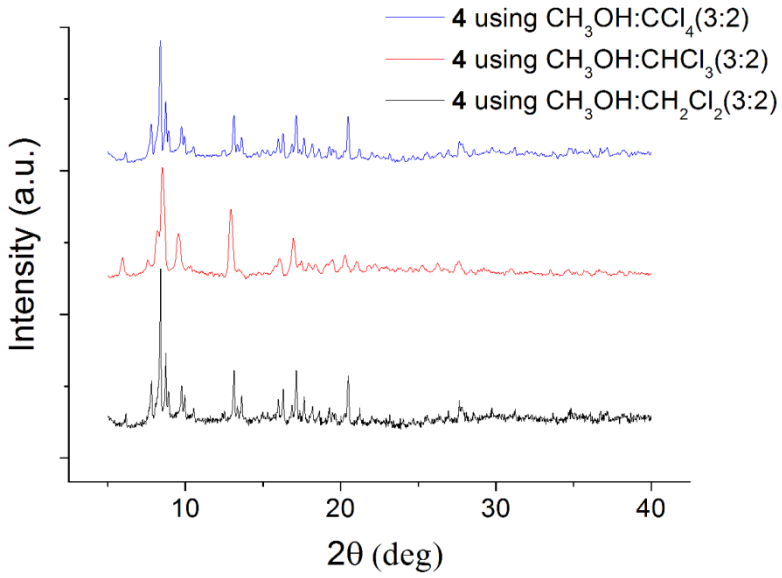

Figure S10. Experimental PXRD patterns of **4** using different chlorinated solvents.

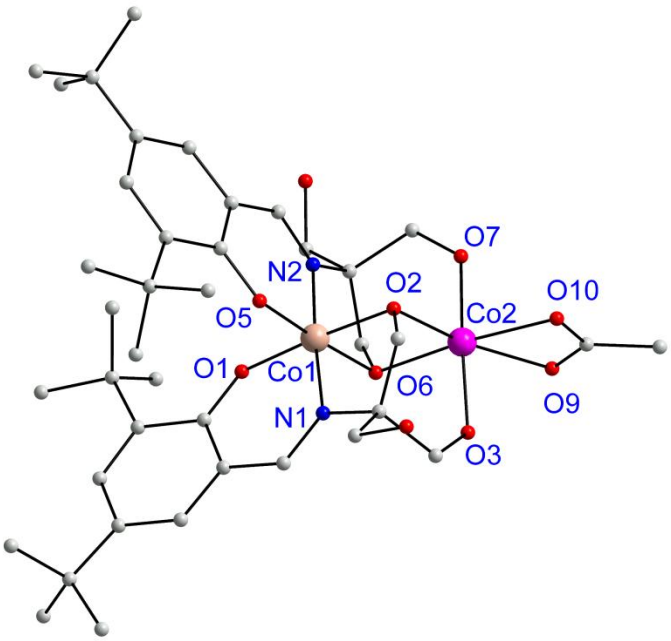

Figure S11. Structure of complex **1** reproduced from CCDC 950084.[1] Hydrogen atoms and solvent molecules are omitted for clarity.

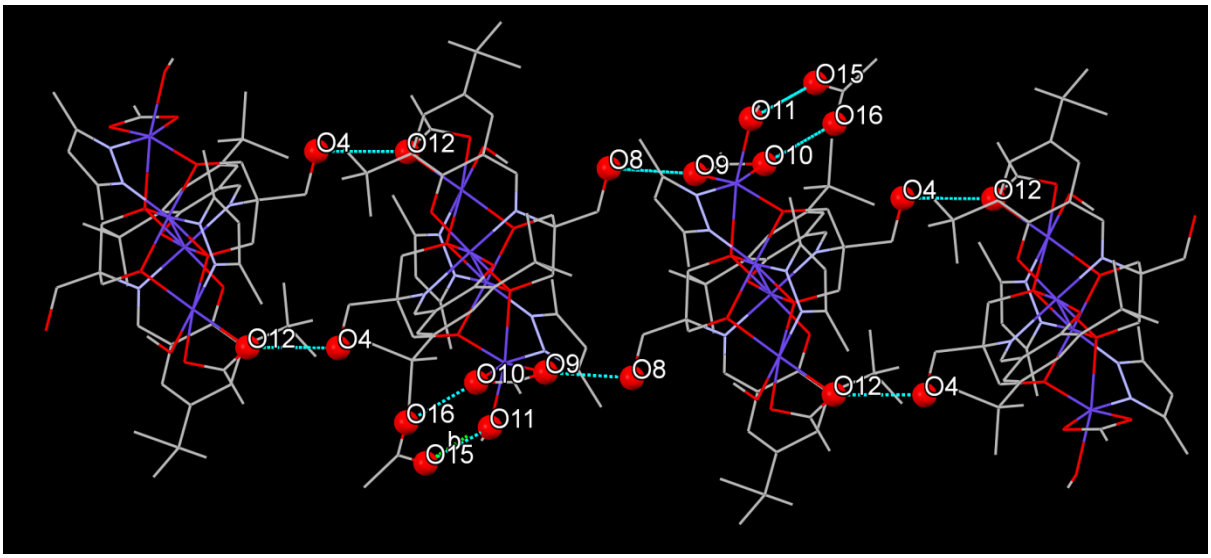

Figure S12. View of a 1D chain linked by intermolecular hydrogen bonding in complex **2.** Hydrogen atoms are omitted for clarity.

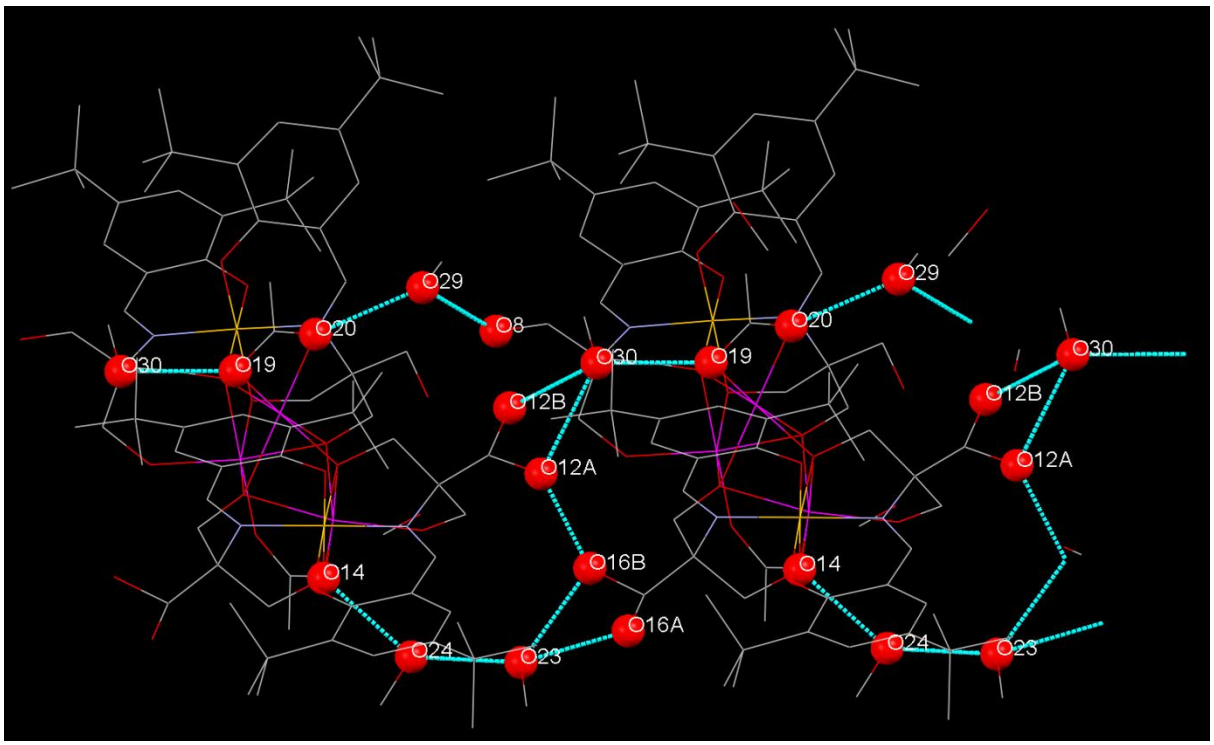

Figure S13. View of a 1D chain linked by intermolecular hydrogen bonding in complex **3.** Hydrogen atoms are omitted for clarity.

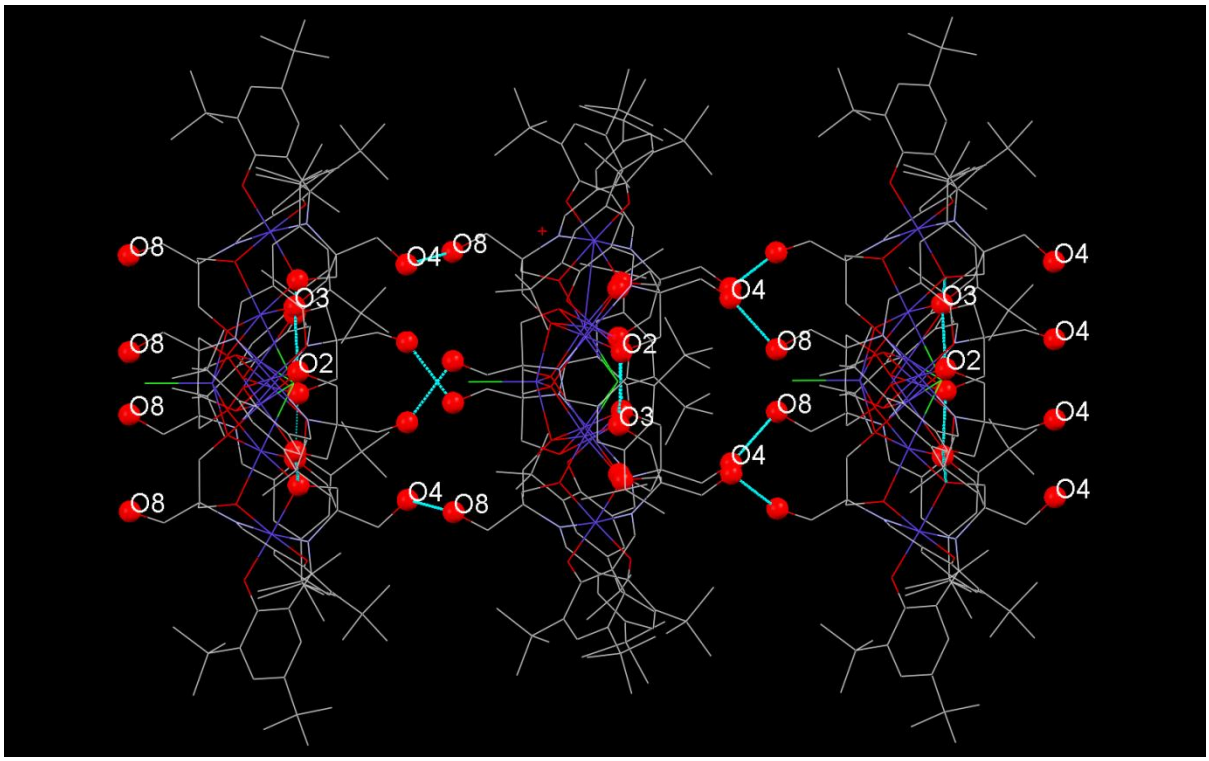

Figure S14. View of a 1D chain linked by intermolecular hydrogen bonding in complex **4.** Hydrogen atoms are omitted for clarity.

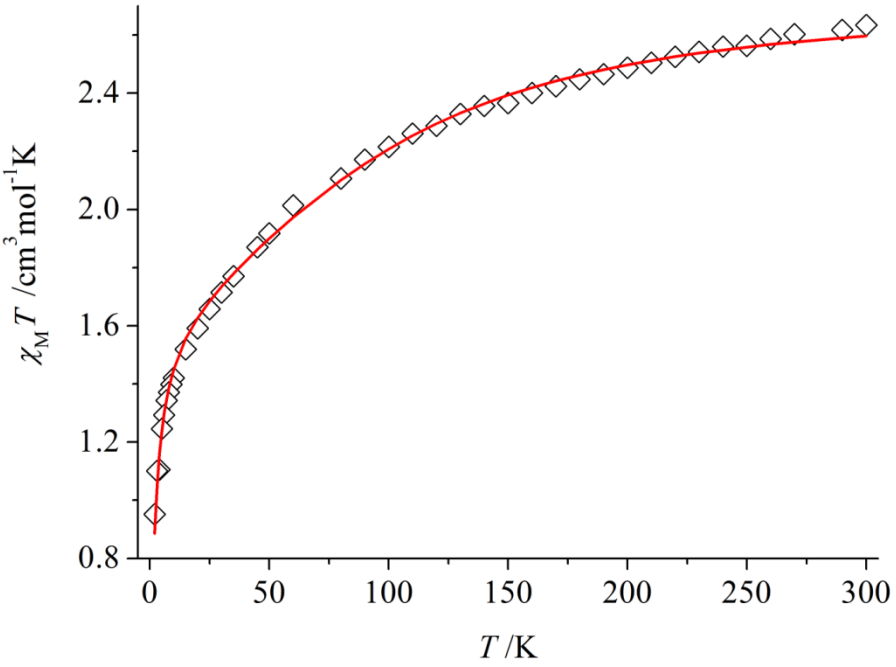

Figure S15. Temperature dependence of $\chi_M T$ under 1 kOe applied dc filed at 2-300 K for a polycrystalline sample of **1** along with simulated fitting of the experimental data shown as red line (parameters: g= 2.402 D= 72.06 cm^{-1}).

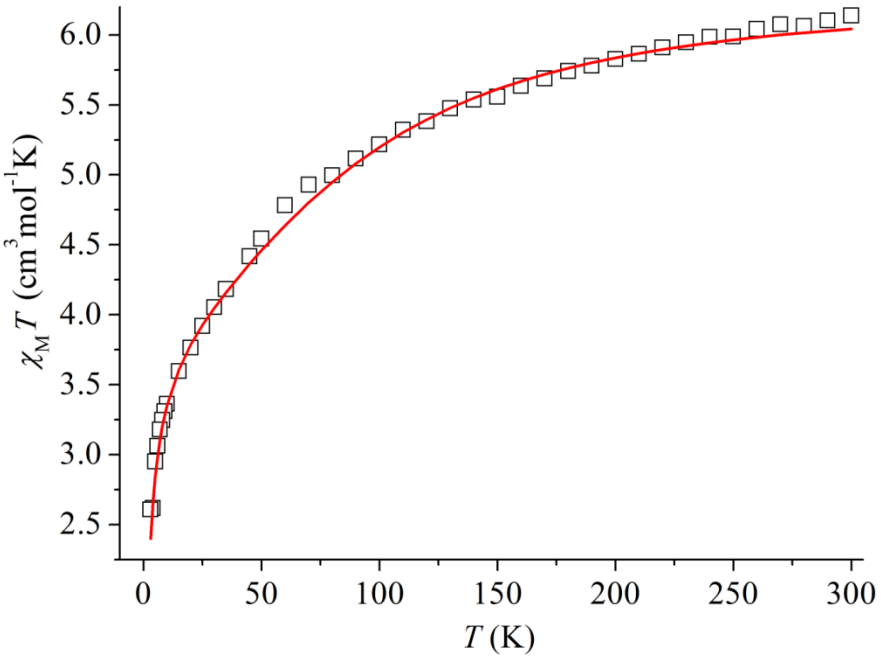

Figure S16. Temperature dependence of $\chi_M T$ under 1 kOe applied dc filed at 2-300 K for a polycrystalline sample of **2** along with simulated fitting of the experimental data shown as red line (parameters: g= 2.585 D= 71 cm^{-1}).

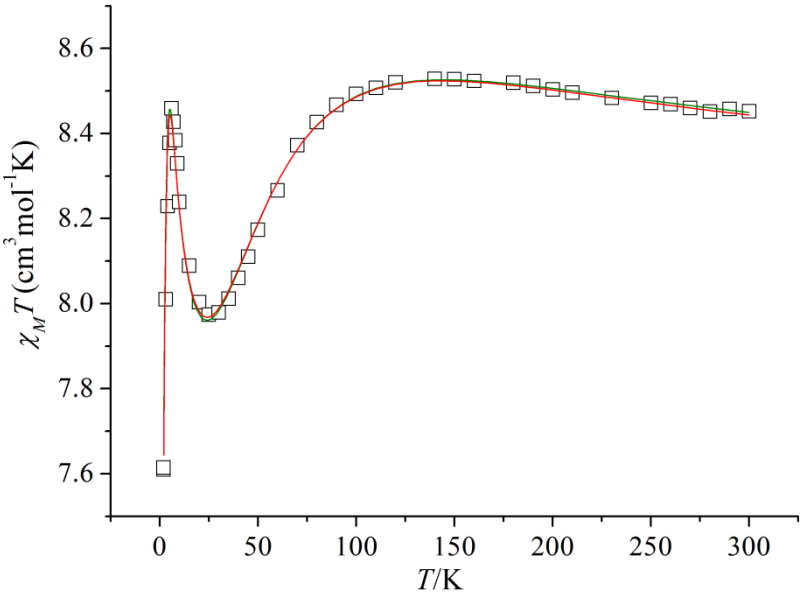

Figure S17. Temperature dependence of $\chi_M T$ under 1 kOe applied dc filed at 2-300 K for a polycrystalline sample of **3** along with simulated fitting of the experimental data shown as solid line [green line (fit1, Table S5), red line(fit2, Table S5)].

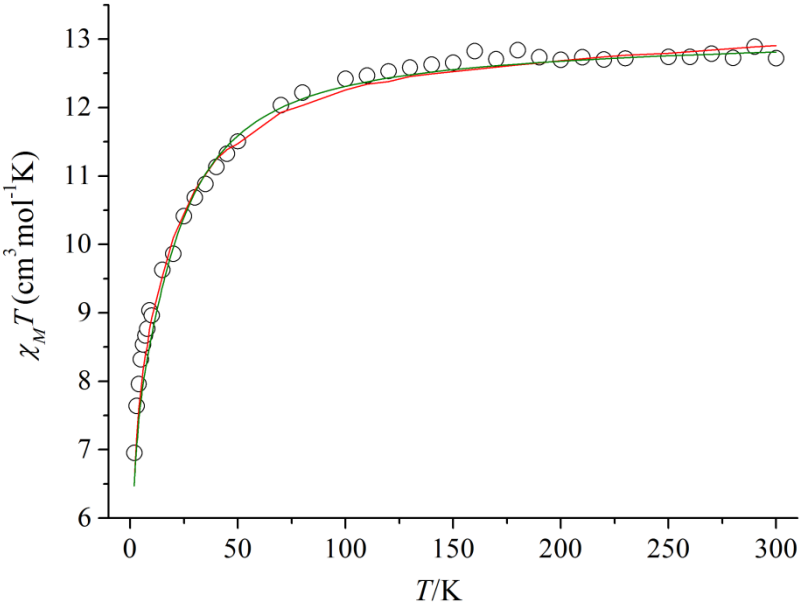

Figure S18. Temperature dependence of $\chi_M T$ under 1 kOe applied dc filed at 2-300 K for a polycrystalline sample of **4** along with simulated fitting of the experimental data shown as solid line [green line (fit 5, Table S6), red line(fit 6, Table S6)].

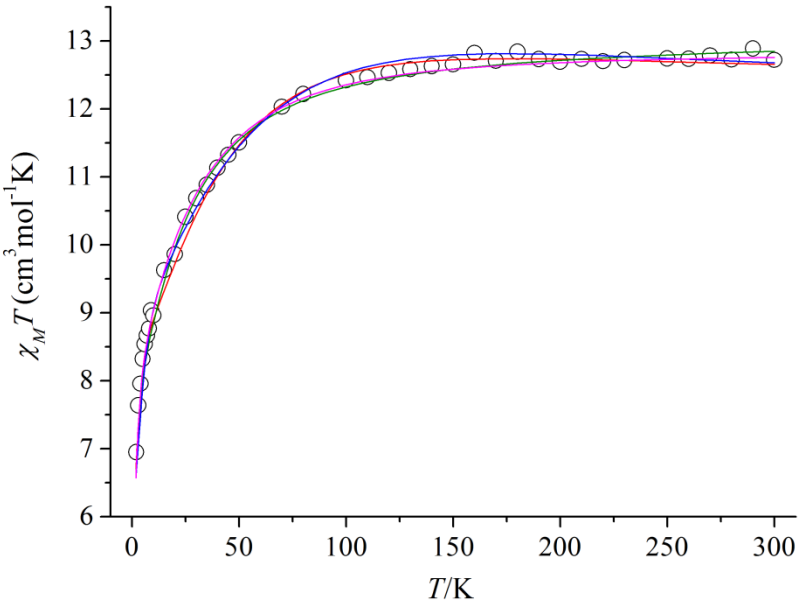

Figure S19. Temperature dependence of $\chi_M T$ under 1 kOe applied dc filed at 2-300 K for a polycrystalline sample of **4** along with simulated fitting of the experimental data shown as red line solid line [blue line (fit1, Table S6), magenta line(fit 2, Table S6), green line (fit 3, Table S6), red line(fit 4, Table S6)].

Table S3 Fitting parameters of $\chi_M T$ *vs* T plot for **1**.

	g	D (cm^{-1})	E/D	T_W	R
1	2.402	72.06	0.699	-1.72	4.99×10^{-4}
2	2.412	64.06	0.919	-1.72	3.15×10^{-4}
3	2.401	86.06	0.489	-1.72	5.20×10^{-4}

Table S4 Fitting parameters of $\chi_M T$ *vs* T plot for **2**.

	g_1	g_2	D_1 (cm^{-1})	D_2 (cm^{-1})	E/D_1	E/D_2	T_W	R
1	2.585	2.585	71	71	0.62	0.62	-1.8	4.24×10^{-4}
2	2.588	2.588	88	88	0.388	0.388	-1.8	3.40×10^{-4}
3	2.59	2.59	60	63	0.848	0.818	-1.68	1.87×10^{-4}

Table S5 Fitting parameters of $\chi_M T$ *vs* T plot for **3**.

	J_1 (cm^{-1})	J_2 (cm^{-1})	g	D (cm^{-1})	R
1	3.64	-1.88	2.414	63.2	9.3×10^{-4}
2	3.76	-1.96	2.412	63.9	8.59×10^{-4}

Table S6 Fitting parameters of $\chi_M T$ *vs* T plot for **4**.

	J_1 (cm^{-1})	J_2 (cm^{-1})	J_3 (cm^{-1})	g	D (cm^{-1})	R
1	15.50	-8.08	-8.65	2.268	74.6	8.89×10^{-4}
2	13.20	-9.35	-10.55	2.352	5.0	3.08×10^{-4}
3	10.78	-8.12	-9.30	2.374	1.5	3.54×10^{-4}
4	13.28	-7.59	-8.22	2.29	55.0	1.38×10^{-4}
5	8.8	-7.81	-8.22	2.39	---	6.48×10^{-4}
6	12.8	-9.51	-11.8	2.37	---	7.59×10^{-4}

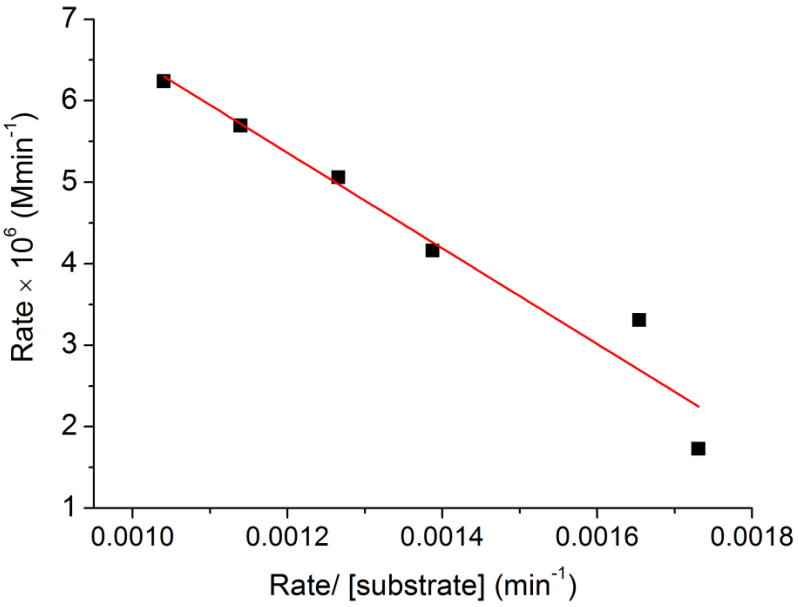

Figure S20. Eadie-Hofstee plot for the oxidation of DTBC catalyzed by **3**.

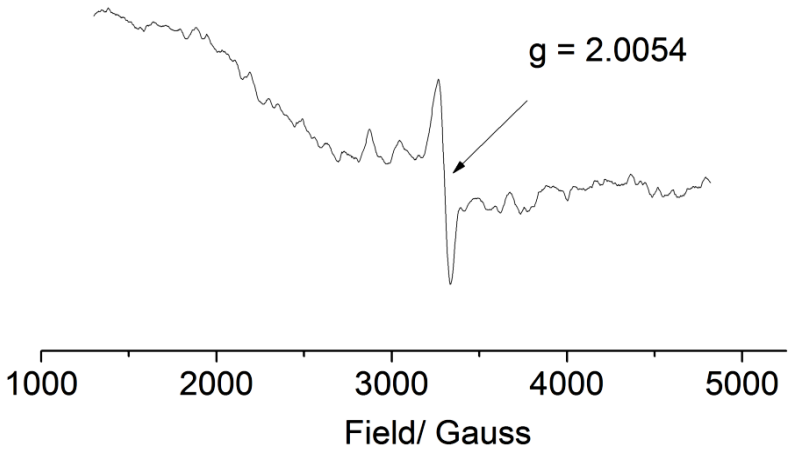

Figure S21. X-Band EPR Spectrum of the mixture of complex **3** and DTBC (1:50) in dimethylformamide at 77K.

Table S7 The kinetic parameters of DTBC oxidation by **3** obtained from different methods

	V_{max} [M min^{-1}]	K_M[M]	k_{cat} [h^{-1}]
Michaelis-Menten	1.20×10^{-5}	0.0056	72.2
Lineweaver-Burk	1.29×10^{-5}	0.0062	77.4
Eadie-Hofstee	1.24×10^{-5}	0.0059	74.4

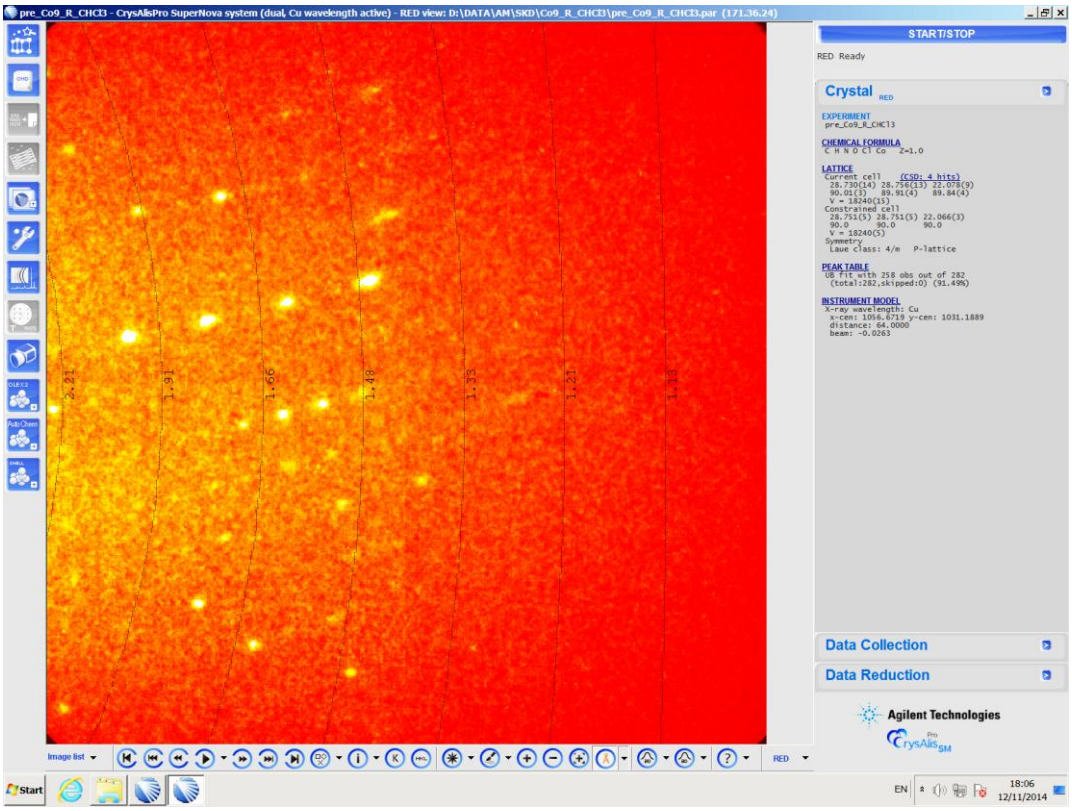

Figure S22. Cell parameters for complex **4** synthesized using CH_3OH and $CHCl_3$ as solvent mixture.

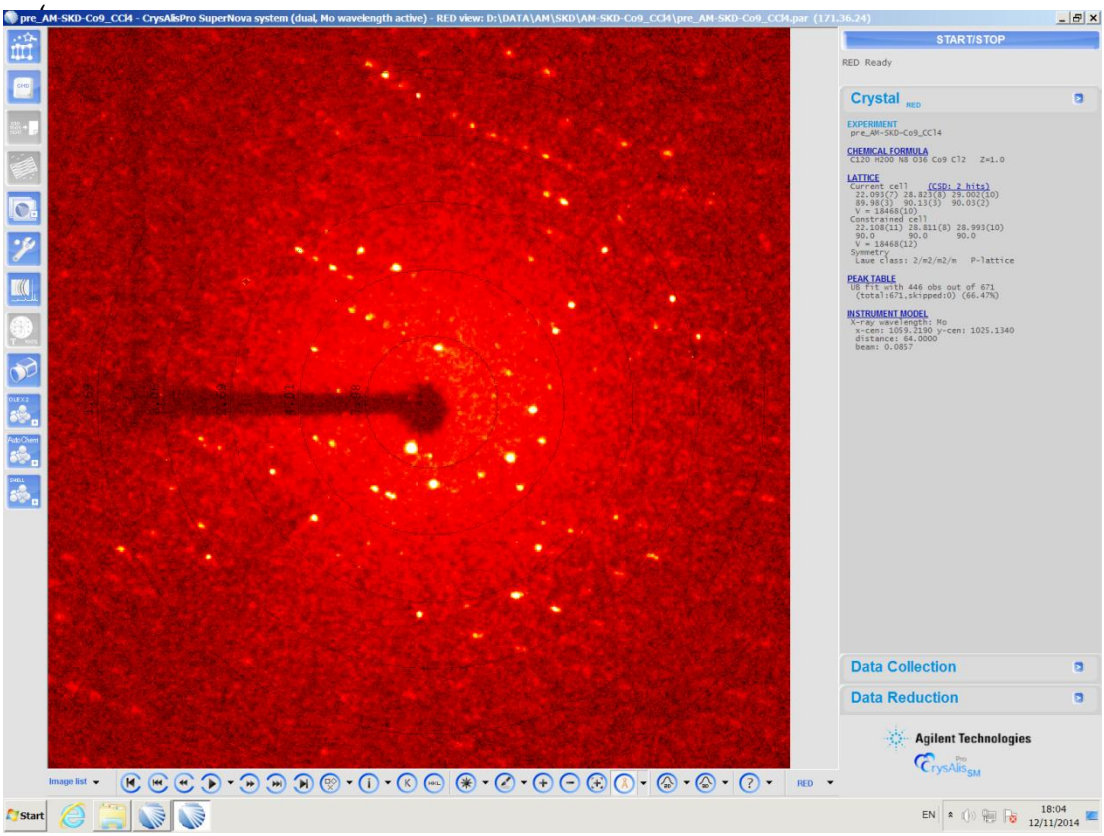

Figure S23. Cell parameters for complex **4** synthesized using CH_3OH and CCl_4 as solvent mixture.

References

1. Dey, S. K.; Mukherjee, A., *New J. Chem.* **2014,** *38*, 4985-4995.